acetate and *p*-chlorophenyl bromoacetate can be used. On the other hand, substitution of the hydrogen atoms on the α-carbon atom will increase steric hindrance. In a series of experiments, Hussey and Newman[28] showed that the yield of β-hydroxy esters dropped when the α-hydrogens were replaced by methyl groups. They attributed this to enolization of the ketone and subsequent reaction of the reagent with the enol form of the ketone. Apparently, this side reaction becomes more important with increased branching of the α-carbon.

All available evidence thus indicates that the Reformatsky reagent is a monomeric, C-metalated species (Ib) in strongly polar solvents and a dimer with bridging $CH_2C(OR)O$ groups in all other solvents.

Acknowledgment. This investigation was supported by the Netherlands Foundation for Chemical Research (SON) with financial aid from the Netherlands Organization for Advancement of Pure Research (ZWO). Data collection was carried out by Dr. A. J. M. Duisenberg.

Registry No. $(BrZnCH_2COO\text{-}t\text{-}Bu{\cdot}THF)_2$, 90528-93-1; $BrZnCH_2COOEt$, 5764-82-9.

Supplementary Material Available: Tables of all positional and thermal parameters and bond lengths and bond angles and a listing of structure factor amplitudes (7 pages). Ordering information is given on any current masthead page.

---

[28] Hussey, A. S.; Newman, M. S. *J. Am. Chem. Soc.* **1948**, *70*, 3024.

Binuclear Phosphido-Bridged WPt, WPd, and WNi Complexes. Crystal and Molecular Structures of $(CO)_4\overline{W(\mu\text{-}PPh_2)_2Pt}(PPh_3)$ and $(CO)_4\overline{W(\mu\text{-}PPh_2)_2Pt}\{CH_3O_2CC{\equiv}CCO_2CH_3\}$

Eric D. Morrison,[†] A. Dale Harley,[†] Michael A. Marcelli,[†] Gregory L. Geoffroy,*[†]
Arnold L. Rheingold,[‡] and William C. Fultz[‡]

Departments of Chemistry, The Pennsylvania State University, University Park, Pennsylvania 16802, and University of Delaware, Newark, Delaware 19711

Received March 12, 1984

The new complexes $(CO)_4\overline{W(\mu\text{-}PPh_2)_2M}(PPh_3)$ (M = Pt, **1**, Pd, **2**, and Ni, **3**) have been prepared by reaction of $Li_2[W(CO)_4(PPh_2)_2]$, generated in situ, with the corresponding $MCl_2(PPh_3)_2$ complex. These complexes have been spectroscopically characterized with the WPt complex **1** further defined by an X-ray diffraction study. It crystallizes in the space group $P2_1/c$ with $a = 11.672$ (2) Å, $b = 18.726$ (3) Å, $c = 19.869$ (3) Å, $\beta = 96.08$ (1)°, $V = 4317$ (1) Å^3, and $Z = 4$. The structure has been refined for the 4491 reflections with $(F_o) > 3\sigma(F_o)$ to R and R_w values of 0.0505 and 0.0495. The W and Pt atoms are bridged by two μ-PPh_2 ligands and joined by a metal–metal bond (2.764 (1) Å). The W is further coordinated by four CO's and the Pt by a PPh_3 ligand. Similar structures are indicated for **2** and **3**. Complexes **1** and **2** show no appreciable reaction with H_2 nor CO under moderate pressures but do react with activated alkynes to quantitatively yield $(CO)_4\overline{W(\mu\text{-}PPh_2)_2M}(MeO_2CC{\equiv}CR)$ (M = Pt, R = CO_2Me, **4**; M = Pt, R = H, **5**; M = Pd, R = CO_2Me, **6**) in which the alkyne has replaced the PPh_3 ligand. Complex **4** crystallizes in the space group $P2_1/n$ with $a = 11.438$ (4) Å, $b = 11.095$ (4) Å, $c = 17.764$ (6) Å, $\beta = 95.55$ (2)°, $V = 3457$ (2) Å^3, and $Z = 4$. The structure refined for the 4098 reflections with $(F_o) > 2.5\sigma(F_o)$ to $R = 0.0431$ and $R_w = 0.0336$. The structure is similar to that of **1** with the alkyne coordinated to Pt such that the alkyne ligand lies nearly in the plane defined by Pt and the two bridging phosphorus atoms. Details of the reaction of **1** with HBF_4 and HCl are also reported.

Heterobimetallic complexes that combine metals with different sets of chemical properties are inherently interesting because they may lead to unusual substrate activation and perhaps unique catalytic chemistry.[1] Particularly interesting are complexes that link metals in groups 4–6 with those in group 8, especially the more active latter metals that readily undergo oxidative-addition/reductive-elimination reactions and which are of catalytic relevance. In other work,[2] we have described such phosphido-bridged WOs, WRh, and WIr complexes, and herein we report new derivatives which link W to Ni, Pd, and Pt, prepared by the general reaction of eq 1. The chemistry of these complexes has been briefly explored, particularly their reactions with alkynes. Also reported are the crystal and molecular structures of complex **1** and its $MeO_2CC{\equiv}CCO_2Me$ derivative, $(CO)_4\overline{W(\mu\text{-}PPh_2)Pt}(MeO_2CC{\equiv}CCO_2Me)$.

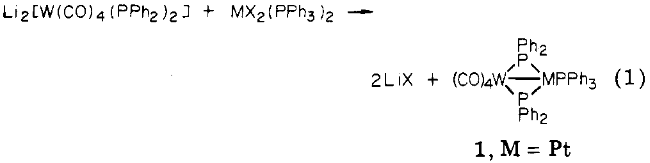

(1)

1, M = Pt
2, M = Pd
3, M = Ni

Experimental Section

$W(CO)_4(PPh_2H)_2$,[2b,3] *cis*-$PtCl_2(PPh_3)_2$,[4] $PdCl_2(PPh_3)_2$,[5] and

---

[†] The Pennsylvania State University.

[‡] University of Delaware.

[1] For leading references see: (a) Roberts, D. A.; Geoffroy, G. L. "Comprehensive Organometallic Chemistry"; Wilkinson, G., Stone, F. G. A., Abel, E. W., Eds.; Pergamon Press: Oxford, 1982; Chapter 40. (b) Stone, F. G. A. *Angew. Chem., Int. Ed. Engl.* **1984**, *23*, 89. (c) Casey, C. P.; Bullock, R. M.; Nief, F. *J. Am. Chem. Soc.* **1983**, *105*, 7574. (d) Ho, S. C. H.; Straus, D. A.; Armantrout, J.; Schaefer, W. P.; Grubbs, R. H. *Ibid.* **1984**, *106*, 2210. (e) Barger, P. T.; Bercaw, J. E. *Organometallics* **1984**, *3*, 278. (f) Finke, R. G.; Gaughan, G.; Pierpont, C.; Noordik, J. H. *Ibid.* **1983**, *2*, 1481.

[2] (a) Breen, M. J.; Geoffroy, G. L.; Rheingold, A. L.; Fultz, W. C. *J. Am. Chem. Soc.* **1983**, *105*, 1069. (b) Breen, M. J.; Shulman, P. M.; Geoffroy, G. L.; Rheingold, A. L.; Fultz, W. C. *Organometallics* **1984**, *3*, 782. (c) Geoffroy, G. L.; Rosenberg, S.; Shulman, P. M.; Whittle, R. R. *J. Am. Chem. Soc.* **1984**, *106*, 1519. (d) Rosenberg, S.; Whittle, R. R.; Geoffroy, G. L. *Ibid.*, in press.

0276-7333/84/2303-1407$01.50/0 © 1984 American Chemical Society

$NiI_2(PPh_3)_2$[6] were prepared according to literature procedures. NiI_2, $W(CO)_6$ (Alfa Ventron Corp.), K_2PtCl_4, K_2PdCl_4 (Colonial Metals), and PPh_3 (Aldrich) were purchased and used as received. Tetrahydrofuran (THF) and hexane were dried by distillation from Na–benzophenone ketyl under N_2, and CH_2Cl_2 was dried by distillation from CaH_2. Unless otherwise specified, manipulations were conducted under a prepurified N_2 atmosphere using standard Schlenk techniques.[7] ^{31}P NMR chemical shifts are relative to external H_3PO_4 with downfield chemical shifts reported as positive.

Preparation of $(CO)_4\overline{W(\mu\text{-}PPh_2)_2Pt}(PPh_3)$, 1. $Li_2[W(CO)_4(PPh_2)_2]$ was generated in situ by reaction of $W(CO)_4(PPh_2H)_2$ (0.333 g, 0.50 mmol) in 15 mL of THF with BuLi (12.8 μL, 1.0 mmol). This solution was added dropwise over 30 min to a slurry of white *cis*-$PtCl_2(PPh_3)_2$ (0.349 g, 0.50 mmol) in 50 mL of THF to give an orange solution. Stirring was continued for 2 h and the THF removed in vacuo. The resultant orange solid was dissolved in 15 mL of 50% CH_2Cl_2/hexane (v/v) and chromatographed on silica gel. An orange band of 1 eluted first, followed by brown and purple bands of presently unidentified compounds. Evaporation of solvent from the first fraction gave complex 1 as reddish orange crystals (0.236 g, 0.210 mmol) in 42.0% yield. Anal. Calcd for $C_{46}H_{35}O_4P_3PtW$: C, 49.17; H, 3.13. Found: C, 49.22; H, 3.26 (Schwarzkopf Microanalytical Laboratory, Woodside, NY).

Preparation of $(CO)_4\overline{W(\mu\text{-}PPh_2)_2Pd}(PPh_3)$, 2. A THF solution of $Li_2[W(CO)_4(PPh_2)_2]$, generated exactly as described above, was added dropwise to a solution of $PdCl_2(PPh_3)_2$ (0.219 g, 0.50 mol) in 50 mL of THF to give a red solution. This was stirred for 1 h and the THF removed in vacuo. The resultant red-brown solid was dissolved in 15 mL of 30% CH_2Cl_2/hexane (v/v) and chromatographed on silica gel. A peach band of an unidentified compound eluted first, followed by a maroon band of 2, and then small orange, red-brown, purple, and red-purple bands of presently unidentified compounds. Rotary evaporation of solvent from the second fraction gave complex 2 as red microcrystals (0.327 g, 0.316 mmol) in 63.2% yield. Anal. Calcd for $C_{46}H_{35}O_4P_3PdW$: C, 53.38; H, 3.41. Found: C, 53.60; H, 3.58.

Preparation of $(CO)_4\overline{W(\mu\text{-}PPh_2)_2Ni}(PPh_3)$, 3. A THF solution containing 0.50 mmol of $Li_2[W(CO)_4(PPh_2)_2]$, generated in situ as described above, was added over 30 min to a dark brown solution of $NiI_2(PPh_3)_2$ (0.419 g, 0.50 mmol) in 35 mL of THF. After the solution was stirred for 2.5 h, the THF was removed in vacuo. The very air-sensitive residue was dissolved in 20 mL of CH_2Cl_2/hexane (30%/70%) and then chromatographed on alumina, Brockman activity 3.1, under N_2. Extensive decomposition occurred during chromatography, but the first brown band that eluted contained complex 3, isolated as an impure solid (0.060 g, ~12% yield) by solvent evaporation. Extensive decomposition persistently occurred upon attempted recrystallization.

Reaction of 1 and 2 with CO and H_2. A solution of 1 (0.104 g, 0.093 mol) in 10 mL of CH_2Cl_2 was placed in a Parr Model 4564 pressure reactor, pressurized with 1350 psi of CO, and allowed to react for 48 h. After the pressure was released, IR analysis showed unchanged 1 as the only carbonyl-containing compound present. Similar results were obtained upon reaction of 1 and 2 with 1750 psi H_2 for 28 h at 22 °C. When complex 2 was allowed to react with CO (1350 psi, 48 h, 22 °C), a small amount of $W(CO)_6$ was detected by IR (ν_{CO} = 1975 cm^{-1}), but 2 was recovered largely unchanged.

Synthesis of $(CO)_4\overline{W(PPh_2)_2Pt}(CH_3O_2CC{\equiv}CCO_2CH_3)$, 4. Complex 1 (0.507 g, 0.451 mmol) was dissolved in air in 10 mL of CH_2Cl_2 in a 4-dram sample vial with a plastic cap. Dimethyl acetylenedicarboxylate (0.208 g, 1.46 mmol) was added to this solution via syringe and allowed to stir for 32 h. The solvent was removed in vacuo, and the light orange residue was chromatographed on silica gel with 30% CH_2Cl_2/hexane as eluant. The first faint orange band to elute was unreacted 1, and this was followed by a bright orange band of 4. Removal of solvent gave 4 as bright orange microcrystals (0.421 g, 0.420 mmol, 93%): ^1H NMR δ 3.6 (s, CH_3). Anal. Calcd for $C_{34}H_{26}O_8P_2PtW$: C, 40.68; H, 2.59. Found: C, 40.74; H, 2.81.

Preparation of $(CO)_4\overline{W(\mu\text{-}PPh_2)_2Pt}(HC{\equiv}CCO_2CH_3)$, 5. Complex 1 (0.060 g, 0.053 mmol) was dissolved in 2 mL of CH_2Cl_2 in a 1-dram sample vial in air. Methyl propiolate (0.095 g, 1.13 mmol) was added via syringe. After the solution was stirred overnight, the solvent was removed in vacuo. Complex 5 was isolated as the second orange band upon silica gel chromatography using 50% CH_2Cl_2/hexane as eluant. The light orange first band is unreacted 1. Evaporation of solvent gave orange microcrystals of 5 (0.035 g, 0.037 mmol) in 70% yield: ^1H NMR δ 3.66 (s, $HC{\equiv}CR$), 3.69 (s, $HC{\equiv}CCO_2CH_3$). Anal. Calcd for $C_{32}H_{24}O_6P_2WPt$: C, 40.09; H, 2.46. Found: C, 40.63; H, 2.56.

Synthesis of $(CO)_4\overline{W(\mu\text{-}PPh_2)_2Pd}(CH_3O_2CC{\equiv}CCO_2CH_3)$, 6. Complex 2 (0.100 g, 0.097 mmol) was dissolved in 2.0 mL of CH_2Cl_2 in a 1-dram sample vial as above. Dimethyl acetylenedicarboxylate (0.289 g, 2.03 mmol) was added and stirred for $^1/_2$ h. The solvent was removed by rotary evaporation in air, and the residue was chromatographed on silica gel with 67% CH_2Cl_2/hexane. The first band to elute was a faint orange band of unreacted 2. The second band contained bright orange 6. Removal of the solvent gave 6 as orange-red microcrystals (0.0651 g, 0.071 mmol) ^1H NMR δ 3.55 (s, CH_3). Anal. Calcd for $C_{34}H_{26}O_8P_2PdW$: C, 44.64; H, 2.87. Found: C, 44.58; H, 3.05.

Reaction of 1 with HBF_4. Complex 1 (0.110 g, 0.098 mmol) in 1.0 g of $CDCl_3$ was treated with 0.10 mL $HBF_4{\cdot}Me_2O$ (0.133 g, 0.993 mmol). Upon shaking, the color changed from deep to light orange. The solution was filtered under N_2 into a 5-mm NMR tube, and the $^{31}P\{^1H\}$ and ^1H NMR spectra were recorded. The IR spectrum of this solution showed ν_{CO} bands at 2070 (vs), 2014 (sh), 1998 (m), and 1967 (s), cm^{-1}, attributed to $[(CO)_4W(\mu\text{-}PPh_2)_2PtH(PPh_3)][BF_4]$, 7. Complex 7 is readily deprotonated by shaking with water to quantitatively regenerate 1. Attempts to isolate 7 by precipitation from $CDCl_3$ or CH_2Cl_2 with hexane persistently resulted in separation of the product as an impure orange oil, 7: ^1H NMR δ −1.70 (dt, J_{PH} = 14.6, 92.8 Hz, J_{PtH} = 775 Hz).

Crystal Structures of Complexes 1 and 4. Crystals of complexes 1 and 4 were grown by slow diffusion of hexane into a CH_2Cl_2 solution of 1 (red crystals) and slow evaporation of a CH_2Cl_2/hexane solution of 4 (orange crystals). Suitable crystals were affixed to a fine glass fiber with a drop of urethane varnish that was also used to coat the crystal to provide a barrier to the atmosphere. The unit cell parameters of both crystals were derived from the angular settings of 25 well-centered reflections ($20° < 2\theta < 28°$) and are provided in Table I along with the parameters of data collection and refinement.

The data were corrected for absorption by an empirical ψ-scan technique (max/min transmission = 0.036/0.015 for 1 and 0.048/0.031 for 4). A profile fitting procedure was applied to the data to improve the precision of the measurement of weak reflections for complex 1. No correction for decay was required for either compound. The monoclinic space groups $P2_1/c$ for 1 and $P2_1/n$ for 4 were uniquely determined from the observed systematic absences. All programs used in the collection and processing of the reflection data are contained in the P3 and SHELXTL (version 4.0) program packages (Nicolet Corp.).

Both structures were solved by the direct-methods routine (SOLV) that provided the locations of the W and Pt atoms; the remaining non-hydrogen atoms were located in subsequent difference Fourier synthesis. In the final cycles of blocked-cascade, least-squares refinement, hydrogen atoms were included as fixed and updated contributions in idealized positions (d(C–H) = 0.96 Å). For complex 1 the carbon atoms of the phenyl rings were refined as rigid groups and all other non-hydrogen atoms were anisotropically refined. All non-hydrogen atoms of complex 4 were refined with anisotropic thermal parameters. In the final cycles, the mean shift/esd (max) was 0.241 for 1 and 0.212 for 4. The highest peak in the final difference map for complex 4 was 0.92 e/Å^3 (1.08 Å from W). Four other difference peaks >0.5 e/Å^3 were also describable as "heavy-metal noise". The final difference map for 1 showed several peaks greater than 1 e/Å^{-3}, but these

---

[3] Treichel, P. M.; Dean, W. K.; Douglas, W. M. *J. Organomet. Chem.* **1972**, *42*, 145.

[4] Bailer, J. C., Jr.; Itatani, H. *Inorg. Chem.* **1965**, *4*, 1618.

[5] Chatt, J.; Mann, F. G. *J. Chem. Soc.* **1939**, 1622.

[6] Venanzi, L. M. *J. Chem. Soc.* **1958**, 719.

[7] Shriver, D. F. "The Manipulation of Air-Sensitive Compounds"; McGraw-Hill: New York, 1969.

Table I. X-ray Diffraction Data for $(CO)_4\overline{W(\mu\text{-}PPh_2)_2Pt}(PPh_3)$, 1, and $(CO)_4\overline{W(\mu\text{-}PPh_2)_2Pt}(CH_3O_2CC{\equiv}CCO_2CH_3)$, 4

	1	4
	Crystal Data	
mol formula	$C_{46}H_{35}O_4P_3PtW$	$C_{34}H_{26}O_8P_2PtW$
mol wt	1091.9	1002.9
space group	$P2_1/c$	$P2_1/n$
a, Å	11.672 (2)	11.438 (4)
b, Å	18.726 (3)	11.095 (4)
c, Å	19.869 (3)	17.764 (6)
β, deg	96.08 (1)	95.55 (2)
V, Å^3	4317 (1)	3457 (2)
ρ(calcd), g cm^{-3}	1.729	2.281
Z	4	4
cryst dimens, mm	0.16 × 0.18 × 0.36	0.24 × 0.31 × 0.36
abs coeff μ(Mo Kα), cm^{-1}	61.35	79.0
temp, °C	27	22
	Intensity Data	
diffractometer	Nicolet R3	Nicolet R3
radiation	Mo Kα (graphite-monochromatized (λ = 0.710 73 Å))	Mo Kα (graphite-monochromatized (λ = 0.710 73 Å))
scan speed, deg min^{-1}	variable; 4.0-20.0	variable, 3.0-20.0
scan type	θ-2θ	ω
scan width	0.9° below 2θ(Kα_1) to 0.9° above 2θ(Kα_2)	0.8° below 2θ(Kα_1) to 0.8° above 2θ(Kα_2)
stds monitored	3/197	3/197
2θ limits, deg	3.0-50.0	4-47.5
reflctns collected	$\pm h,+k,+l$	$\pm h,+k,+l$
no. of reflctns collected	6446	5329
unique reflctns	5355	4885
unique reflctns used	4491, $(F_o) > 3.0\sigma(F_o)$	4098, $(F_o) > 2.5\sigma(F_o)$
weighting factor g[a]	0.000 91	
$R(F)$[b]	0.0505	0.0431
$R(F_w)$[c]	0.0495	0.0336
GOF	1.243	1.407

[a] Weight = $[\sigma^2(F) + |g|(F^2)]^{-1}$. [b] $R = \Sigma[|F_o| - |F_c|]/\Sigma|F_o|$. [c] $R_w = [\Sigma w^{1/2}(|F_o| - |F_c|)]/\Sigma w^{1/2}|F_o|$.

were generally less than 1.10 Å from the metal atoms. Final positional parameters for 1 and 4 are given in Tables II and III, respectively. Anisotropic thermal parameters, complete lists of bond lengths and angles, and the structure factors are given in the supplementary material.

Results and Discussion

Synthesis of $(CO)_4\overline{W(\mu\text{-}PPh_2)_2M}(PPh_3)$ (M = Ni, Pd, Pt) Complexes. In earlier work we had shown that bis(phosphido)-bridged WIr, WRh, and WOs complexes are readily prepared in good yields by the reaction of $Li_2[W(CO)_4(PPh_2)_2]$ (eq 2) with appropriate Rh and Ir halide complexes.[2] Binuclear WPt, WPd, and WNi complexes also result in modest to good yields from similar reactions with the corresponding MX_2L_2 (M = Pt, Pd, Ni) complexes (eq 3). Chromatography of solutions following

$$W(CO)_4(PPh_2H)_2 + 2\ BuLi \rightarrow 2BuH + Li_2[W(CO)_4(PPh_2)_2] \quad (2)$$

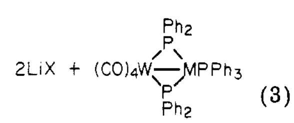

1, M = Pt, X = Cl (42%)
2, M = Pd, X = Cl (63%)
3, M = Ni, X = I (~12%)

these reactions showed that several additional compounds were formed (see Experimental Section), but so far only products 1–3 have been positively characterized. The WPt and WPd complexes 1 and 2 were isolated in pure form, but the WNi complex 3 proved too unstable to be analytically pure. Complex 3 decomposes upon SiO_2 and Al_2O_3 chromatography and rapidly turns into a brown oil upon air exposure.

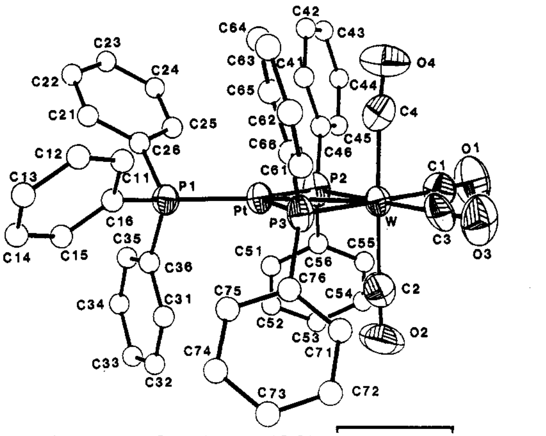

Figure 1. An ORTEP drawing of $(CO)_4\overline{W(\mu\text{-}PPh_2)_2Pt}(PPh_3)$, 1. Hydrogen atoms have been omitted, and the carbon atoms of the phenyl rings are shown as spheres, radius 0.25 Å, for clarity. The thermal ellipsoids for the remaining atoms are shown at the 50% probability level.

Spectroscopic Characterization of Complexes 1, 2, and 3. Infrared and ^{31}P NMR spectral data for all the new complexes reported herein are given in Table IV. The WPt complex 1 has been fully characterized by a single-crystal X-ray diffraction study (Figure 1). The similarity of the IR and ^{31}P NMR spectra for 1, 2, and 3 suggests that all three compounds have similar structures, that depicted in eq 3 and Figure 1. The ^{31}P NMR spectra are particularly informative with each complex showing downfield resonances due to the μ-PPh$_2$ groups with ^{31}P–^{183}W coupling and a separate resonance attributable to the PPh$_3$ ligand that does not couple to ^{183}W. The downfield position of the μ-PPh$_2$ resonances implies the presence of a metal–metal bond in each compound,[8] consistent with the

Table II. Atomic Positional Parameters (×10^4) and Temperature Factors (Å^2 × 10^3) for 1

atom	*x*	*y*	*z*	U^a
W	3561 (1)	6085 (1)	4163 (1)	42 (1)
Pt	2806 (1)	7480 (1)	4002 (1)	41 (1)
P(1)	2202 (3)	8612 (2)	3921 (2)	45 (1)
P(2)	1665 (3)	6629 (2)	4370 (2)	49 (1)
P(3)	4608 (3)	7162 (2)	3793 (2)	46 (1)
C(1)	2824 (12)	5176 (7)	4411 (7)	61 (5)
C(2)	4148 (14)	6264 (7)	5143 (7)	72 (6)
C(3)	5012 (13)	5556 (6)	4043 (7)	55 (5)
C(4)	3013 (11)	5882 (7)	3196 (7)	54 (5)
O(1)	2350 (11)	4656 (5)	4539 (6)	104 (5)
O(2)	4488 (12)	6346 (6)	5703 (5)	111 (6)
O(3)	5855 (8)	5241 (5)	3986 (6)	85 (4)
O(4)	2735 (10)	5706 (6)	2641 (4)	93 (5)
C(11)	3580 (10)	9063 (5)	2972 (6)	83 (7)
C(12)	4254 (10)	9545 (5)	2651 (6)	116 (10)
C(13)	4431 (10)	10234 (5)	2909 (6)	123 (10)
C(14)	3935 (10)	10440 (5)	3487 (6)	135 (11)
C(15)	3261 (10)	9958 (5)	3807 (6)	108 (9)
C(16)	3083 (10)	9269 (5)	3550 (6)	59 (6)
C(21)	563 (8)	9342 (4)	3028 (4)	55 (5)
C(22)	−534 (8)	9434 (4)	2687 (4)	74 (6)
C(23)	−1409 (8)	8949 (4)	2784 (4)	93 (8)
C(24)	−1186 (8)	8371 (4)	3221 (4)	89 (7)
C(25)	−88 (8)	8279 (4)	3562 (4)	67 (6)
C(26)	786 (8)	8764 (4)	3466 (4)	44 (4)
C(31)	2993 (8)	8936 (6)	5230 (5)	94 (8)
C(32)	2910 (8)	9169 (6)	5890 (5)	120 (9)
C(33)	1865 (8)	9431 (6)	6070 (5)	153 (11)
C(34)	904 (8)	9460 (6)	5589 (5)	158 (10)
C(35)	988 (8)	9227 (6)	4929 (5)	129 (8)
C(36)	2032 (8)	8965 (6)	4750 (5)	57 (5)
C(41)	333 (8)	6467 (5)	3167 (5)	73 (6)
C(42)	−632 (8)	6257 (5)	2738 (5)	94 (8)
C(43)	−1545 (8)	5913 (5)	3003 (5)	111 (9)
C(44)	−1493 (8)	5779 (5)	3697 (5)	135 (10)
C(45)	−528 (8)	5989 (5)	4125 (5)	87 (7)
C(46)	385 (8)	6334 (5)	3861 (5)	56 (5)
C(51)	1020 (9)	7333 (4)	5493 (4)	74 (6)
C(52)	762 (9)	7392 (4)	6160 (4)	93 (8)
C(53)	779 (9)	6787 (4)	6571 (4)	110 (8)
C(54)	1055 (9)	6123 (4)	6314 (4)	192 (12)
C(55)	1313 (9)	6064 (4)	5646 (4)	183 (12)
C(56)	1296 (9)	6669 (4)	5236 (4)	58 (5)
C(61)	6144 (7)	7229 (4)	2806 (4)	67 (6)
C(62)	6420 (7)	7296 (4)	2142 (4)	86 (7)
C(63)	5545 (7)	7350 (4)	1609 (4)	76 (6)
C(64)	4394 (7)	7337 (4)	1740 (4)	66 (6)
C(65)	4118 (7)	7271 (4)	2403 (4)	62 (5)
C(66)	4993 (7)	7217 (4)	2936 (4)	50 (5)
C(71)	6630 (10)	7081 (4)	4684 (5)	74 (6)
C(72)	7576 (10)	7376 (4)	5074 (5)	93 (8)
C(73)	7733 (10)	8115 (4)	5091 (5)	98 (8)
C(74)	6943 (10)	8558 (4)	4717 (5)	103 (9)
C(75)	5997 (10)	8263 (4)	4326 (5)	82 (6)
C(76)	5840 (10)	7524 (4)	4310 (5)	55 (5)

[a] Equivalent isotropic *U* defined as one third of the trace of the orthogonalized U_{ij} tensor.

structural results for 1 (W–Pt = 2.764 (1) Å). Literature data show that downfield (δ 50–300) resonances are generally found for μ-PPh$_2$ ligands bridging metal–metal bonds whereas upfield (δ +50 to −200) resonances occur when these ligands bridge two metals not joined by a metal–metal bond.[8] However, some exceptions have been found to this correlation so caution must be exercised in its use.[9]

Table III. Atom Coordinates (×10^4) and Temperature Factors (A^2 × 10^3) for 4

atom	*x*	*y*	*z*	U^a
Pt	3734 (1)	5736 (1)	2097 (1)	49 (1)
W	4602 (1)	4663 (1)	3199 (1)	51 (1)
P(1)	5681 (2)	5605 (2)	2497 (1)	52 (1)
P(2)	2592 (2)	4838 (2)	2637 (1)	54 (1)
O(1)	844 (7)	6241 (6)	652 (5)	137 (4)
O(2)	4269 (8)	7804 (4)	815 (6)	132 (5)
O(3)	838 (6)	6965 (4)	1665 (4)	91 (3)
O(4)	5145 (7)	6723 (5)	564 (5)	107 (4)
O(11)	4827 (7)	3412 (4)	1901 (4)	89 (3)
O(12)	3513 (21)	3481 (15)	4305 (13)	109 (11)
O(13)	4151 (7)	5913 (5)	4453 (4)	98 (4)
O(14)	7082 (7)	4116 (6)	3948 (5)	120 (4)
C(1)	2600 (8)	6417 (5)	1432 (5)	56 (4)
C(2)	3673 (9)	6616 (5)	1323 (5)	58 (4)
C(3)	1365 (9)	6526 (6)	1186 (6)	71 (4)
C(4)	4359 (9)	7118 (6)	884 (6)	72 (4)
C(5)	−385 (8)	7064 (7)	1513 (7)	107 (6)
C(6)	5934 (12)	7131 (8)	110 (8)	146 (9)
C(11)	4766 (8)	3857 (6)	2364 (5)	60 (4)
C(12)	3906 (8)	3888 (6)	3896 (5)	65 (4)
C(13)	4307 (8)	5480 (5)	3991 (6)	64 (4)
C(14)	6181 (10)	4332 (7)	3698 (6)	73 (4)
C(21)	6395 (8)	6466 (5)	2922 (5)	52 (3)
C(22)	6720 (8)	6516 (6)	3689 (5)	71 (4)
C(23)	7253 (13)	7206 (11)	3991 (10)	101 (8)
C(24)	7493 (14)	7799 (9)	3559 (11)	93 (7)
C(25)	7177 (10)	7736 (6)	2811 (7)	97 (6)
C(26)	6648 (9)	7066 (5)	2485 (6)	80 (5)
C(31)	6662 (7)	5267 (5)	1827 (5)	53 (3)
C(32)	6256 (9)	5059 (5)	1093 (5)	66 (4)
C(33)	7033 (12)	4800 (7)	585 (6)	89 (6)
C(34)	8215 (11)	4746 (6)	809 (7)	83 (5)
C(35)	8596 (10)	4937 (7)	1532 (7)	86 (5)
C(36)	7872 (9)	5213 (6)	2034 (6)	75 (5)
C(41)	1430 (7)	5168 (6)	3187 (5)	57 (4)
C(42)	740 (9)	4652 (7)	3521 (6)	84 (5)
C(43)	−120 (14)	4911 (11)	3957 (9)	100 (7)
C(44)	−307 (16)	5694 (14)	4056 (10)	122 (10)
C(45)	349 (17)	6212 (10)	3699 (9)	115 (9)
C(46)	1226 (10)	5951 (6)	3281 (6)	87 (5)
C(51)	1963 (8)	4084 (5)	1998 (5)	54 (4)
C(52)	1678 (8)	4260 (5)	1244 (5)	60 (4)
C(53)	1198 (9)	3702 (6)	752 (6)	70 (4)
C(54)	985 (11)	2963 (7)	1002 (8)	76 (6)
C(55)	1270 (10)	2787 (6)	1746 (7)	90 (5)
C(56)	1749 (9)	3339 (6)	2243 (6)	72 (4)

[a] Equivalent isotropic *U* defined as one third of the trace of the orthogonalized U_{ij} tensor.

Reactivity of Complexes 1 and 2. The reactivity of the WPt and WPd complexes 1 and 2 has been briefly examined, but the WNi complex 3 proved too unstable to study further. The results are summarized in the following paragraphs.

1. With H_2 and CO. No significant detectable reaction was observed when complexes 1 and 2 were separately kept under pressures of H_2 and CO for 48 h, even though stable adducts or dimer disruption products might have been anticipated. A small amount (<5%) of $W(CO)_6$ did form in the reaction of 2 with CO, but these results overall demonstrate the general ability of μ-PPh$_2$ ligands to retard or prevent fragmentation of such polynuclear compounds.[10]

2. With Alkynes. The WPt and WPd complexes 1 and 2 react with activated alkynes to yield products in which the alkyne has replaced the terminal PPh$_3$ ligand (eq 4). Spectroscopic monitoring showed that these reactions go essentially to completion when the reactants are allowed to stand in air-saturated CH_2Cl_2 solutions for several hours.

---

[8] (a) Carty, A. J. *Adv. Chem. Ser.* **1982,** *No. 196,* 163. (b) Carty, A. J.; MacLaughlin, S. A.; Taylor, N. J. *J. Organomet. Chem.* **1981,** *204,* C27. (c) Petersen, J. L.; Stewart, R. P., Jr. *Inorg. Chem.* **1980,** *19,* 186. (d) Garrou, P. E. *Chem. Rev.* **1981,** 229.

[9] Jones, R. A.; Wright, T. C.; Atwood, J. C.; Hunter, W. E. *Organometallics* **1983,** *2,* 470.

[10] However, see: ref 2c and Harley, A. D.; Guskey, G. J.; Geoffroy, G. L. *Organometallics* **1983,** *2,* 53.

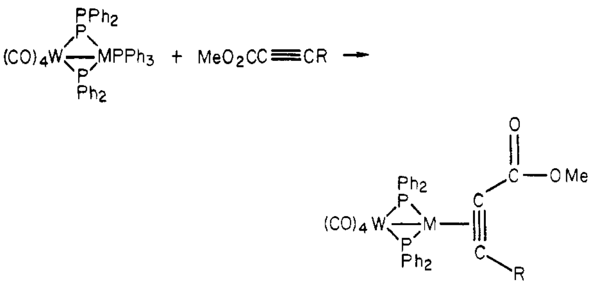

(4)

4, M = Pt, R = CO_2Me (93%)
5, M = Pt, R = H (70%)
6, M = Pd, R = CO_2Me (73%)

Some loss of compound does occur upon chromatography; isolated yields are given in eq 4.

These new complexes have been spectroscopically characterized, and complex **4** has been further defined by a complete single-crystal X-ray diffraction study (Figure 3). The spectroscopic data (Table IV) are similar for the three compounds and imply similar structures. The IR spectra show a 15–30 cm^{-1} blue-shift in the bands of the $W(CO)_4$ portion of the molecules upon replacing the electron-donating PPh_3 ligand with the electron-accepting alkyne ligands. Also observable in the IR spectra of **4** and **6** are weak bands at 1707 and 1705 cm^{-1}, respectively, which may be attributed to the ester carbonyl stretch of the coordinated alkynes. The ^{31}P NMR spectrum of each shows the expected downfield resonance for the μ-PPh_2 ligands with ^{183}W and ^{195}Pt coupling consistent with the structures indicated in eq 4. The methyl propiolate complex **5** shows two downfield μ-PPh_2 resonances (Table IV). This is consistent with the structure determined for complex **4** in which the alkyne ligand is in the same plane as the two μ-PPh_2 ligands and thus the latter are inequivalent due to the asymmetry of the alkyne.

The mechanism by which these substitution reactions proceed is unknown. However, it should be noted that all these reactions were conducted in air-saturated solutions and that ^{31}P NMR analysis of the reaction mixture from the combination of **1** with $MeO_2CC{\equiv}CCO_2Me$ showed that *all* of the original PPh_3 ligand had been converted to $O{=}PPh_3$. Since $Pt(PPh_3)_3$ is a known catalyst for the oxidation of PPh_3 to $O{=}PPh_3$,[11] it is possible that O_2 facilitates the removal of PPh_3 to open a site for alkyne coordination. Studies are in progress to further define the course of these reactions and to try to isolate possible O_2 adducts of **1**. Only activated alkynes appear to react with **1** and **2** since $PhC{\equiv}CPh$, $PhC{\equiv}CH$, and $CH_3C{\equiv}CH$ gave no detectable reaction under comparable conditions.

3. With HBF_4 and HCl. The WPt complex **1** reacts rapidly with HBF_4 to yield the protonated product **7** (eq 5). The ^{31}P NMR spectrum of **7** shows two downfield resonances for inequivalent μ-PPh_2 ligands and a separate resonance for the PPh_3 ligand with ^{31}P–^{31}P and ^{195}Pt–^{31}P coupling constants consistent with the structure depicted in eq 5. Complex **7** is readily deprotonated by shaking $CDCl_3$ or CH_2Cl_2 solutions with H_2O to immediately and quantitatively regenerate **1**. Complex **1** also reacts with HCl to give the chloride salt of **7**.

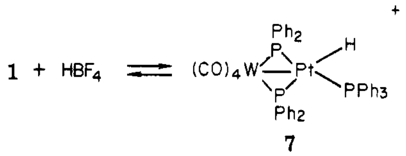

(5)

7

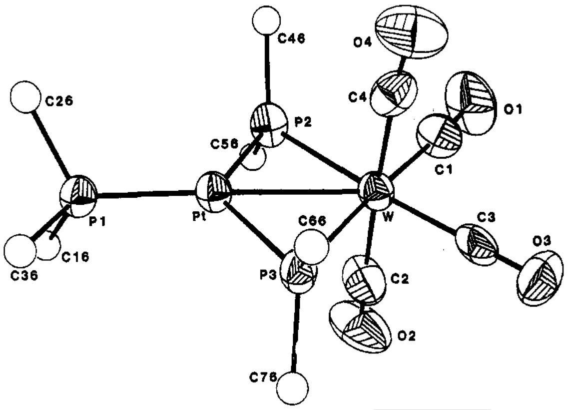

Figure 2. Perspective drawing of $(CO)_4\overline{W(\mu\text{-}PPh_2)_2Pt}(PPh_3)$, **1**, showing only the non-hydrogen atoms and the first carbon atom of each ring.

Crystal and Molecular Structure of $(CO)_4\overline{W(\mu\text{-}PPh_2)_2Pt}(PPh_3)$, 1. An ORTEP drawing of **1** giving the atom labeling scheme is shown in Figure 1 with a blowup of the central core of the molecule shown in Figure 2. Relevant bond angles and distances are set out in Table V. The tungsten center has an octahedral coordination geometry, if we neglect the Pt atom, and the Pt center has a trigonal-planar arrangement of the three phosphorus ligands. The $WPt(\mu\text{-}PPh_2)_2$ core of the molecule is essentially planar with a dihedral angle of 2.2° between the P(2)–W–P(3) and P(2)–Pt–P(3) planes. The W–Pt distances of 2.764 (1) Å falls within the range found for WPt distances in other crystallographically characterized molecules (e.g., $PtW(\mu\text{-}CC_6H_4CH_3)(CO)_2(PMe_2Ph)_2Cp$, 2.751 (1) Å,[12] $PtW(\mu\text{-}C(OMe)Ph)(CO)_5(PMe_3)_2$, 2.861 (1) Å,[13] and $Pt_2W(\mu\text{-}C(OMe)Ph)_2(CO)_6(PMe(t\text{-}Bu)_2)_2$, 2.828 (2) and 2.832 (2) Å).[14]

The question of direct metal–metal bonding in doubly bridged compounds is still controversial since the bonding interaction between the metals may take place through orbitals involving the bridging atoms.[15] We do not wish to enter that controversy but would like to be able to assess the relative oxidation states of the metals in **1**. The relatively short PtW distance in **1** does imply some degree of metal–metal interaction since it is well-known that short M–M distances are not imposed by μ-PPh_2 bridging ligands as these can span distances as great as 3.7 Å.[16] A metal–metal bond is required to give each metal a satisfactory electron count: 18 for W and 16 for Pt.

With the assumption of a metal–metal interaction of some type, â priori three possible descriptions exist. There are two anionic ligands ($2PPh_2$) in **1**, and thus a total metal oxidation state of +2 must be accounted for. The molecule could be described as having a direct covalent single metal–metal bond between $d^5W(I)$ and $d^9Pt(I)$ centers (**1a**),

---

(11) Sen, A.; Halpern, J. *J. Am. Chem. Soc.* **1977**, *99*, 8337 and references therein.

(12) Ashworth, T. V.; Howard, J. A. K.; Stone, F. G. A. *J. Chem. Soc., Dalton Trans.* **1980**, 1609.

(13) Ashworth, T. V.; Howard, J. A. K.; Laguna, M.; Stone, F. G. A. *J. Chem. Soc., Dalton Trans.* **1980**, 1593.

(14) Ashworth, T. V.; Berry, M.; Howard, J. A. K.; Laguna, M.; Stone, F. G. A. *J. Chem. Soc., Dalton Trans.* **1980**, 1615.

(15) (a) Mason, R.; Mingos, D. M. P. *J. Organomet. Chem.* **1973**, *50*, 53. (b) Teo, B. K.; Hall, M. B.; Fenske, R. F.; Dahl, L. F. *Ibid.* **1974**, *70*, 413. (c) Granozzi, G.; Benoni, R.; Tondello, E.; Casarin, M.; Aim, S.; Osello, D. *Inorg. Chem.* **1983**, *22*, 3899.

(16) See, for example: (a) Rosen, R. P.; Hoke, J. B.; Whittle, R. R.; Geoffroy, G. L.; Hutchinson, J. P.; Zubieta, J. A. *Organometallics* **1984**, *3*, 846. (b) Ginsburg, R. E.; Rothrock, R. K.; Finke, R. G.; Collman, J. P.; Dahl, L. F. *J. Am. Chem. Soc.* **1979**, *101*, 6550.

Table IV. Infrared and ^{31}P NMR Spectral Data

complex	ν_{CO},[a] cm^{-1}	$^{31}P\{^1H\}$[b] $\delta(\mu\text{-}PPh_2)$	$\delta(PPh_3)$	$J_{^{31}P-^{31}P}$	$J_{^{31}P-^{183}W}$	$J_{^{31}P-^{195}Pt}$
1 (WPt)	2032 (s), 1940 (s, sh), 1925 (s, br)	173.8 (d)	47.7 (t)	47.6	154.6	2659 (μ-PPh_2) 5148 (PPh_3)
2 (WPd)	2041 (s), 1952 (s, br), 1931 (s, br)	165.2 (d)	23.4 (t)	15.2	83.9	
3 (WNi)	2027 (s), 1941 (s), 1923 (vs)	128.6 (d)	39.4 (t)	24.5	80.9	
4	2056 (s), 1969 (s), 1946 (vs), 1808 (w), 1707 (w)	187.1 (s)			166.8	2269
5	2053 (s), 1968 (s), 1947 (vs)	188.7 (d) 190.8 (d)		83.3	*c*	2316 2354
6	2056 (s), 1973 (nm), 1948 (s), 1875 (w), 1705 (w)	202.5 (s)			185.6	
7	2070 (s), 2014 (sh), 1998 (m), 1967 (s)	210.0 (dd, P_1) 215.0 (dd, P_2)	20.1 (dd)	P_1-PPh_3, 140.3 P_2-PPh_3, 10.6 P_1-P_2, 17.7	*c*	985 (P_1) 1507 (P_2) 3319 (PPh_3)

[a] CH_2Cl_2 (1, 2, 4-6); $CDCl_3$ (7); THF (3). [b] C_6D_6 (1-3); $CDCl_3$ (4-7). [c] Not sufficiently resolved.

Table V. Selected Bond Distances (Å) and Angles (deg) for $(CO)_4\overline{W(\mu\text{-}PPh_2)_2Pt}(PPh_3)$ with Estimated Standard Deviations

	Bond Distances		
Pt-W	2.764 (1)	P(1)-C(16)	1.811 (11)
Pt-P(1)	2.234 (3)	P(1)-C(26)	1.820 (9)
Pt-P(2)	2.249 (3)	P(1)-C(36)	1.804 (11)
Pt-P(3)	2.266 (4)	P(2)-C(46)	1.800 (10)
W-P(2)	2.509 (4)	P(2)-C(56)	1.818 (10)
W-P(3)	2.507 (3)	P(2)-C(66)	1.810 (9)
W-C(1)	1.993 (14)	P(3)-C(76)	1.808 (11)
W-C(2)	2.021 (13)	P(2)···P(3)	3.865 (4)
W-C(3)	1.998 (14)	C(2)-O(2)	1.151 (17)
W-C(4)	1.995 (14)	C(3)-O(3)	1.164 (17)
C(1)-O(1)	1.160 (17)	C(4)-O(4)	1.164 (16)
	Bond Angles		
Pt-W-P(2)	50.2 (1)	W-Pt-P(1)	177.4 (1)
Pt-W-P(3)	50.6 (1)	W-Pt-P(2)	59.0 (1)
Pt-W-C(1)	134.1 (4)	W-Pt-P(3)	58.8 (1)
Pt-W-C(2)	91.5 (4)	P(1)-Pt-P(2)	120.2 (1)
Pt-W-C(3)	135.9 (4)	P(1)-Pt-P(3)	121.9 (1)
Pt-W-C(4)	90.2 (4)	P(2)-Pt-P(3)	117.8 (1)
P(2)-W-P(3)	100.8 (1)		
P(2)-W-C(1)	84.0 (4)		
P(2)-W-C(2)	89.4 (5)	Pt-P(2)-W	70.8 (1)
P(2)-W-C(3)	173.8 (4)	Pt-P(3)-W	70.6 (1)
P(2)-W-C(4)	92.1 (4)		
P(3)-W-C(1)	179.8 (4)		
P(3)-W-C(2)	91.3 (4)	W-C(1)-O(1)	176 (1)
P(3)-W-C(3)	85.3 (4)	W-C(2)-O(2)	178 (1)
P(3)-W-C(4)	89.3 (4)	W-C(3)-O(3)	178 (1)
C(1)-W-C(2)	90.8 (5)	W-C(4)-O(4)	174 (1)
C(1)-W-C(3)	89.9 (5)		
C(1)-W-C(4)	88.9 (5)		
C(2)-W-C(3)	89.5 (6)		
C(2)-W-C(4)	178.2 (5)		
C(3)-W-C(4)	88.8 (5)		

a polar donor–acceptor bond between $d^6W(O)$ and $d^8Pt(II)$ centers (**1b**), or a polar donor–acceptor bond in the opposite direction between $d^4W(II)$ and $d^{10}Pt(0)$ centers (**1c**).

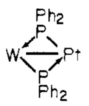

1a

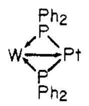

1b

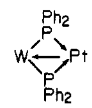

1c

These descriptions only reflect the relative energies of the metal orbitals involved in the bonding: in **1a** the interacting orbitals on each metal would have nearly the same energy; in **1b**, the Pt orbitals would lie higher in energy; and in **1c**, the W orbitals would be highest. Unfortunately, the available data does not allow a definitive conclusion to be drawn as to which description is appropriate for **1**. Sensitive indicators of metal oxidation states are the stretching frequencies of coordinated CO's. The ν_{CO} bands in **1** at 2032 (s), 1940 (s), and 1925 (s) cm^{-1} are slightly higher in energy than the corresponding vibrations of the W(O) precursor complex $W(CO)_4(PPh_2H)_2$ at 2020 (s), 1917 (sh), 1905 (vs), and 1893 (sh) cm^{-1}. This implies a partial oxidation of W in the binuclear complex although it does not appear to be extensive. Given this fact and the initial oxidation states in the W(O) and Pt(II) precursor complexes, formulation **1b** appears most reasonable.

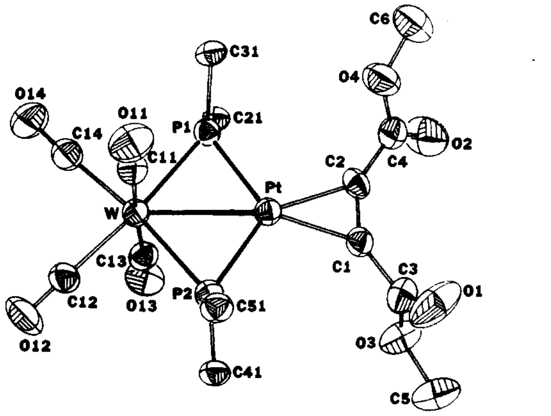

Figure 3. An ORTEP drawing of $(CO)_4\overline{W(\mu\text{-}PPh_2)_2Pt}(MeO_2CC{\equiv}CCO_2Me)$, **4**. For clarity, only the phenyl carbon atoms attached to phosphorus are shown.

Crystal and Molecular Structure of $(CO)_4\overline{W(\mu\text{-}PPh_2)_2Pt}(MeO_2CC{\equiv}CCO_2Me)$, 4. An ORTEP drawing of **4** is shown in Figure 3. For clarity, the phenyl carbons, except for those attached to phosphorus, have been omitted. As in **1**, the tungsten center has an octahedral coordination geometry, if we neglect the Pt atom, and the Pt center is coordinated by two phosphorus atoms and the alkyne ligand. The $WPt(\mu\text{-}PPh_2)$ core of the molecule is nearly planar with a dihedral angle of 6.0° between the P(1)-W-P(2) and P(1)-Pt-P(2) planes, as illustrated by the view shown in Figure 4. The alkyne carbon atoms are also nearly coplanar with these atoms; the dihedral angle between the Pt-C(1)-C(2) and Pt-W-P(1)-P(2) planes is 7.5°. Such an arrangement appears to be the most sterically favorable as it places the alkyne substituents between the phosphorus phenyl rings. The PtW distance of 2.795 (1) Å is similar to that in **1** (2.764 (1) Å).

The metal-metal bonding/oxidation state discussion

Table VI. Relevant Bond Lengths (Å) and Bond Angles (deg) in $(CO)_4\overline{W(\mu\text{-}PPh_2)_2Pt}(MeO_2CC{\equiv}CCO_2Me)$

Bond Lengths

Pt-W	2.795 (1)	Pt-P(1)	2.282 (3)
Pt-P(2)	2.285 (3)	Pt-C(1)	2.034 (9)
Pt-C(2)	2.035 (9)	W-P(1)	2.443 (3)
W-P(2)	2.435 (3)	W-C(11)	2.048 (10)
W-C(12)	2.028 (10)	W-C(13)	2.034 (10)
W-C(14)	2.014 (11)	P(1)-C(21)	1.812 (9)
P(1)-C(31)	1.809 (10)	P(2)-C(41)	1.814 (10)
P(2)-C(51)	1.820 (9)	O(1)-C(3)	1.177 (13)
O(2)-C(4)	1.183 (12)	O(3)-C(3)	1.323 (13)
O(3)-C(5)	1.409 (12)	O(4)-C(4)	1.298 (14)
O(4)-C(6)	1.446 (17)	O(11)-C(11)	1.127 (12)
O(12)-C(12)	1.130 (27)	O(13)-C(13)	1.132 (12)
O(14)-C(14)	1.143 (14)	C(1)-C(2)	1.306 (14)
C(1)-C(3)	1.450 (14)	C(2)-C(4)	1.441 (14)

Bond Angles

W-Pt-P(1)	56.4 (1)	W-Pt-P(2)	56.2 (1)
P(1)-Pt-P(2)	112.5 (1)	W-Pt-C(1)	161.1 (3)
P(1)-Pt-C(1)	141.8 (3)	P(2)-Pt-C(1)	105.6 (3)
W-Pt-C(2)	161.0 (3)	P(1)-Pt-C(2)	104.6 (3)
P(2)-Pt-C(2)	142.8 (3)	C(1)-Pt-C(2)	37.5 (4)
Pt-W-P(1)	51.1 (1)	Pt-W-P(2)	51.2 (1)
P(1)-W-P(2)	102.2 (1)	P(2)-W-C(11)	89.1 (3)
P(1)-W-C(11)	89.3 (3)	P(2)-W-C(11)	86.2 (3)
P(2)-W-C(12)	136.3 (3)	P(1)-W-C(12)	171.8 (3)
P(2)-W-C(12)	85.4 (3)	C(11)-W-C(12)	94.1 (4)
P(2)-W-C(13)	87.8 (3)	P(1)-W-C(13)	91.5 (3)
P(2)-W-C(13)	89.2 (3)	C(11)-W-C(13)	175.4 (4)
C(12)-W-C(13)	85.7 (4)	Pt-W-C(14)	137.3 (3)
P(1)-W-C(14)	86.2 (3)	P(2)-W-C(14)	170.4 (3)
C(11)-W-C(14)	89.4 (4)	C(12)-W-C(14)	86.3 (4)
C(13)-W-C(14)	95.2 (4)	Pt-P(1)-W	72.4 (1)
C(4)-O(4)-C(6)	119.3 (9)	Pt-P(2)-W	72.5 (1)
P(2)-C(1)-C(3)	142.8 (7)	C(3)-O(3)-C(6)	116.7 (8)
P(2)-C(2)-C(1)	72.2 (6)	Pt-C(1)-C(2)	71.3 (6)
C(1)-C(2)-C(4)	143.5 (9)	Pt-C(1)-C(3)	142.8 (7)
O(1)-C(3)-C(1)	126.3 (10)	C(2)-C(1)-C(3)	145.5 (9)
O(2)-C(4)-O(4)	121.8 (10)	Pt-C(2)-C(4)	145.1 (7)
O(4)-C(4)-C(2)	111.4 (9)	O(1)-C(3)-O(3)	121.8 (10)
W-C(12)-O(12)	177.1 (15)	O(3)-C(3)-C(1)	111.8 (8)
W-C(14)-O(14)	176.1 (9)	O(2)-C(4)-C(2)	126.8 (10)
		W-C(22)-O(11)	178.4 (8)
		W-C(13)-O(13)	177.3 (9)

given above for 1 applies equally well to 4. The ν_{CO} bands of 4 (2056, 1969, 1946 cm^{-1}) show a much more pronounced blue-shift as compared to $W(CO)_4(PPh_2H)_2$ (2020, 1917, 1905, 1893 cm^{-1}) than does 1, and this implies a greater degree of oxidation of W in 4 than in 1. It is significant that a ligand substitution on the Pt end of the molecule is so strongly felt by the W center and its ligands at the other end.

Summary

In this study we have continued to demonstrate the utility of the "bridge-assisted" synthetic approach[1a] for directing the synthesis of phosphido-bridged compounds. In this strategy the ligand that ends up bridging between the metals plays the important role of bringing the metals together. In these examples, the anionic PPh_2 ligands of the $[W(CO)_4(PPh_2)_2]^{2-}$ reagent brings the separated metals together by substituting for X^- on the $MX_2(PPh_3)_2$ reagent. As illustrated by the lack of reaction under H_2 and CO pressures, the WPt and WPd complexes 1 and 2 are quite robust, although the WNi complex 3 is thermally unstable and extremely air sensitive. The Pt and Pd ends of 1 and 2 are reactive, however, as the PPh_3 ligand can be replaced readily by activated alkynes and probably by other substrates as well. Such reactions will be the subject of future studies.

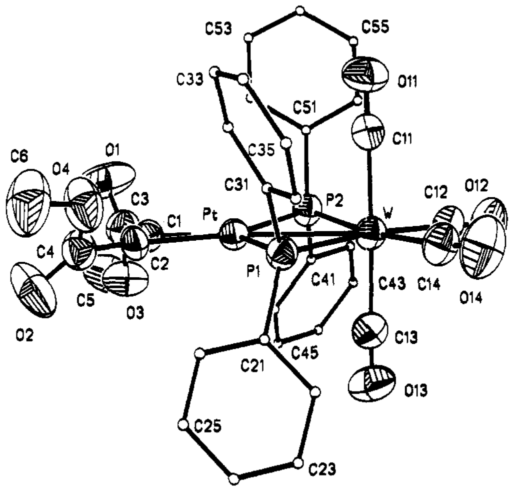

Figure 4. An ORTEP drawing of $(CO)_4\overline{W(\mu\text{-}PPh_2)_2Pt}(MeO_2CC{\equiv}CCO_2Me)$, 4. Hydrogen atoms have been omitted, and the carbon atoms of the phenyl rings are shown as spheres, of arbitrary size, for clarity. Thermal ellipsoids are drawn at the 40% probability level.

Acknowledgment. We gratefully acknowledge the National Science Foundation (CHE 8201160) for support of this research.

Registry No. 1, 90867-32-6; 2, 90867-33-7; 3, 90885-96-4; 4, 90867-34-8; 5, 90867-35-9; 6, 90885-97-5; 7, 90867-37-1; $Li_2[W(CO)_4(PPh_2)_2]$, 68829-50-5; *cis*-$PtCl_2(PPh_3)_2$, 15604-36-1; *trans*-$PdCl_2(PPh_3)_2$, 14056-88-3; $NiI_2(PPh_3)_2$, 14057-03-5; $W(CO)_4(PPh_2H)_2$, 70505-43-0; W, 7440-33-7; Pt, 7440-06-4; Pd, 7440-05-3; Ni, 7440-02-0.

Supplementary Material Available: Tables of anisotropic thermal parameters, hydrogen atom coordinates and temperature factors, complete lists of bond lengths and angles, and structure factors (60 pages). Ordering information is given on any current masthead page.